JOURNAL OF MATERIALS SCIENCE 25 (1990) 1268–1274

Zirconia by the gel route

A. AYRAL, T. ASSIH, M. ABENOZA, J. PHALIPPOU
Laboratoire de Science des Matériaux Vitreux, Université de Montpellier II, France
A. LECOMTE, A. DAUGER
Ecole Nationale Supérieure de Céramique Industrielle, Limoges, France

Zirconia gels are synthesized by hydrolysis of zirconium n-propoxide under acidic conditions in an alcoholic medium. The Raman spectroscopy shows that the hydrolysis of the alkoxide occurs as soon as the reactants are mixed. Small angle X-ray scattering analyses allow us to propose a mechanism which takes account of the formation of the gel backbone. The gelation is related to the aggregation of primary clusters which are very quickly produced in the solution. The mean size of these clusters is 2 nm. The wet gel shows a fractal structure. The xerogel is demonstrated to be an amorphous compound of zirconium hydroxyoxide. This compound retains nitrate anions which are present in the solution. The structural evolution of the thermally treated xerogels is followed using X-ray diffraction and Raman spectroscopy.

1. Introduction

The zirconium oxide ZrO_2 is an attractive oxide with respect to the volumetric expansion related to the tetragonal–monoclinic transformation. It is presently used to improve the mechanical properties of zirconia or composite ceramic materials [1].

The gel route and the use of organometallic precursors are doubly attractive for zirconia. Doped homogeneous mixtures can be prepared and the microstructure of the final product can be controlled by a suitable selection of the synthesis parameters. Little information is available concerning the hydrolysis of the zirconium alkoxides. Bradley and Carter have studied the first steps of the hydrolysis of zirconium alkoxides [2, 3]. They observed the formation of polymeric oxide alkoxides. Yoldas [4] has shown the effects of various parameters such as the alkoxide concentration, the water/alkoxide molar ratio or the addition of acids on the morphology of the produced solid and on its thermal evolution. Contrary to the case of the silicon alkoxides and the silica gels the mechanisms which lead to the gelation of hydrolysed solutions of zirconium alkoxide are not known. Thus, this study is performed to better understand the gelation phenomenon in these zirconium alkoxide solutions. The structural evolution of the solution up to the gel is carried out using Raman spectroscopy and small angle X-ray scattering (SAXS). Raman spectroscopy was previously demonstrated as a very useful tool for studying the gelation and the gel structure [5]. SAXS allows the growth of polymeric species during the gelation step to be followed [6].

Otherwise, the effect of the synthesis conditions on the structure, the texture and, further, the thermal evolution of the gels remain to be researched and as a consequence this paper is devoted to these investigations.

2. Experimental procedure

2.1. Sample preparation

2.1.1. Synthesis

The gel synthesis is made from zirconium n-propoxide, water and nitric acid. The solvent is 2-propanol. The order of reactant addtion is: alkoxide, solvent, acid (65 weight % HNO_3 aqueous solution), water.

After stirring, the solution is poured into a glass tube. This tube is hermetically closed and introduced in an oven maintained at 40° C. After gelation the tube is removed from the oven.

The different compositions of the solutions are reported on the ternary diagram (Fig. 1). For a given composition, the weight percents are calculated with respect to reactants only:

$$\text{wt \% } Zr(O^nPr)_4 + \text{wt \% } H_2O + \text{wt \% } HNO_3 = 100$$

The dilution ratio r_d is the ratio in weight of 2-propanol to reactants.

The series a to d corresponds to a constant water percent (quasi constant molar concentration of water) and r_d value equal to 1.4. The other series A to E corresponds to a constant alkoxide percent (quasi constant molar concentration of alkoxide) and r_d value equal to 1.35.

2.1.2. Drying and thermal treatments

The wet gels are slowly dried at room temperature. This drying treatment causes the gels to break into small pieces. The structural evolution of the xerogels is studied on samples thermally treated for 2 h at a given temperature.

2.2. Experimental methods

2.2.1. Raman spectroscopy

The spectra are recorded on a triple monochromator spectrometer using an argon ion laser at 514.5 nm.

0022–2461/90 $03.00 + .12

Gel	t (h)
A	21
B	5
C	4
D	0h 15min
E	a few sec.
a	120
b	3h 45min
c	instantaneously
d	instantaneously

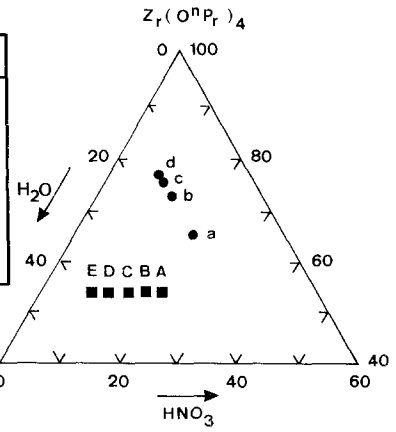

Figure 1 Compositions and gelation times:

The wet gels are studied *in situ* in their closed tube. The syneresis liquid is analysed in the supernatant liquid part. Raman spectra of pure reactants and assumed by-products of hydrolysis were also recorded.

Scattering light is analysed at 90° of the incident beam in the study of the reactants and the wet gels. In the case of the dried gels and the thermally treated gels, powdered gel platelets are analysed using back-scattered light. X-ray diffraction analysis was performed on the same platelets.

2.2.2. Small angle X-ray scattering

To follow the structural evolution of the gelifying mixtures aliquots were sampled from solution containers for different given times. Wet gels were analysed according to the same technique. The tight cell has "mylar" windows. The sample thickness is about 500 μm.

The measurements are performed using a point-like small angle camera (Cu$K\alpha$-quartz monochromator). The scattered intensities are counted with a position-sensitive proportional counter. Experimental results were corrected for parasite scattering and normalized to equivalent sample thickness, incident intensity and counter efficiency. It must be noted that the SAXS curves are translated on intensity axis for clarity. Thus the reported intensity I corresponds to αI_m where α is a constant and I_m, the real measured value.

3. Results and discussion

3.1. The gelation

By Raman spectroscopy we have followed the structural evolution of a solution with time. The first spectrum is recorded just after the reactants are mixed. The spectrum is not modified during the whole gelation process. The relative intensities of the diffusion bands remain apparently constant.

Fig. 2e shows the wet gel spectrum. It mainly shows the characteristic diffusion bands of 2-propanol (820, 955, 1124 cm^{-1}) (Fig. 2b) and 1-propanol (468, 864, 891, 972, 1060, 1073, 1107 cm^{-1}) (Fig. 2c).

1-propanol is a by-product of the hydrolysis reaction:

$$Zr(O^nC_3H_7)_4 + xH_2O \rightarrow Zr(O^nC_3H_7)_{4-x}(OH)_x + x\,{}^nC_3H_7OH$$

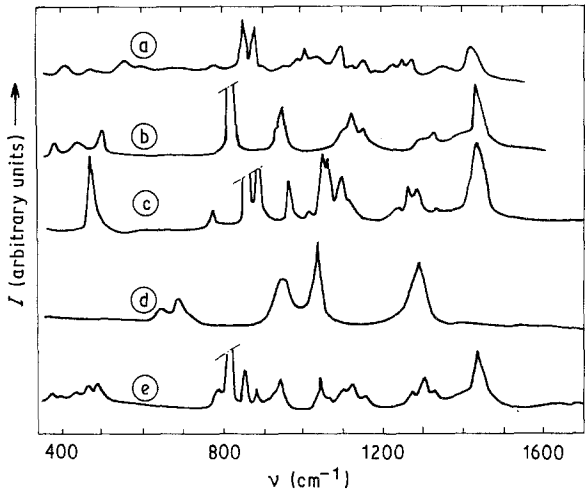

Figure 2 Raman spectra: a) zirconium n-propoxyde; b) 2-propanol; c) 1-propanol; d) concentrated nitric acid; e) wet gel a.

However, because diffusion bands of the alkoxide (Fig. 2a) are found for the same frequencies as the main diffusion bands of 1-propanol (Fig. 2c), it is not possible to claim that the alkoxide is fully hydrolysed. We can ascertain that 1-propanol is well produced by the hydrolysis reaction and not due to an exchange reaction with the solvent. Effectively the Raman spectrum of a mixture zirconium n-propoxide–2-propanol does not exhibit any characteristic band of 1-propanol. Therefore the Raman study of the gelation indicates that zirconium alkoxide hydrolysis mainly occurs at the beginning of the gelation process.

SAXS experiments are performed on composition B as a function of time (Figs 3 and 4). The electronic radius of gyration R_G is determined from the plot of Log I against H^2 where I is the scattered intensity and H, the scattering vector. For the small angles, the Guinier approximation $I \alpha \exp(-H^2R_G^2/3)$ is available and R_G is evaluated from the slope of the curve. In the first instant (B_0–Fig. 3) the measured radius of gyration is 1.2 nm. It corresponds to the size of the clusters which are produced by the hydrolysis reaction.

For higher values of wave vector (H), the scattered intensity decays as a power law $I(H) \alpha H^{-p}$. For dense particles or aggregates having a smooth surface p is equal to 4 as expected from the classical Porod law. When the p value is in the range 3–4, the scattering

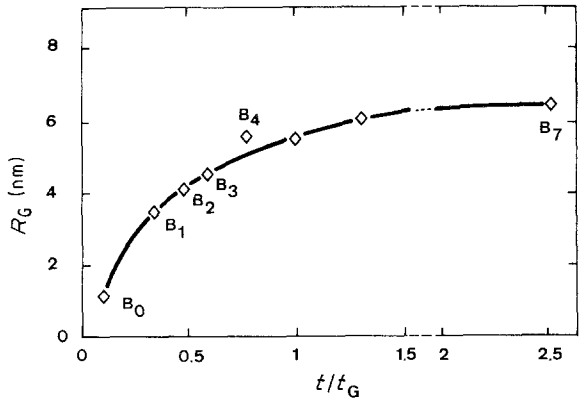

Figure 3 Radius of gyration versus reduced time t/t_G for composition B (t_G = gelation time).

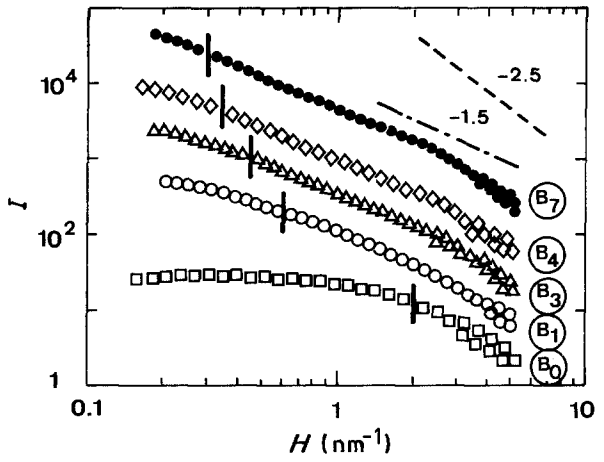

Figure 4 $I = f(H)$ for composition $B(I \equiv 2/R_G$; for analysis times, see Fig. 3).

unit exhibits a surface fractal structure. If p is lower than 3 the scattering unit is a mass fractal object [7] and p is also its fractal dimension. The lower limit of the Porod region is usually defined by $H = 2R_G^{-1}$. For the curve B_0 (Fig. 4), in the Porod region, the slope is close to -2.5. This value displays the polymeric mass fractal structure of the initial cluster.

The radius of gyration increases with reduced time (Fig. 3). It is noteworthy that for short times the radius of gyration has a physical signification and near the gel time it rather corresponds to a correlation length.

For reduced times higher than 0.1, two slopes can be observed on the log–log plots (Fig. 4). For H values more than $2\,nm^{-1}$, the slope is about -2.5 as for curve B_0. With H in the range $2R_G^{-1}$ to $2\,nm^{-1}$, the slope is quite constant and equal to -1.5. This value of the slope indicates that the gel can be considered as a mass fractal structure.

The scattering curves show two slopes for all the studied gels. The change in slope is always situated around $2\,nm^{-1}$. From the experimental results the gelation process can be interpreted as resulting from the aggregation of polymeric clusters, these primary clusters being produced very quickly in the solution during the hydrolysis stage. Furthermore the fractal dimension of the cluster aggregate, 1.5, indicates that the gel growth more probably occurs by a cluster–cluster aggregation type mechanism [7]. It is noteworthy that the structure of the primary clusters does not change during the gelation process.

3.2. The wet gels

Raman analyses of wet gels are performed as soon as they are obtained but also when aged for several months. These spectra exhibit as previously described the diffusion bands of 1-propanol and 2-propanol. However, more or less intense bands can be observed at 600, 800, 1320 and 1710 cm^{-1}. Moreover, for samples which require long gelation time (>24 h) these bands appear immediately after the gelation. For other samples ageing is necessary to permit the bands to be observed.

With ageing, syneresis occurs which causes the liquid to go out of the pores. The Raman spectrum of

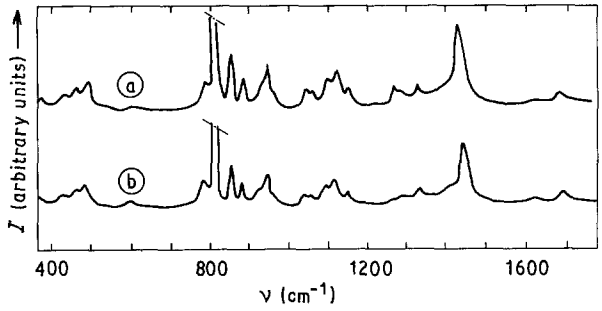

Figure 5 Raman spectra: a) syneresis liquid of gel B; b) 1-propanol, 2-propanol, and nitric acid mixture.

the syneresis liquid (Fig. 5a) is practically identical to that of the wet gel (Fig. 5b) and shows the same diffusion bands.

To explain the origin and the evolution of these bands we have prepared a mixture of 1-propanol, 2-propanol, and nitric acid. Their respective chosen amounts are those expected to be found in composition B. The mixture is refluxed at 75° C for two hours and the Raman spectrum is then recorded. This spectrum corresponds to that of the syneresis liquid (see Figs 5a and b). Thus the observed diffusion bands are mainly due to the products of a reaction between the alcohols and the nitric acid. This reaction being thermally activated, we can explain the behaviour difference between the gels as a function of their gelation time. Thus the appearance and the evolution of these bands are not related to the structural evolution of the solid part of the gel.

To determine the bands generated by the solid part of the gel we have performed another analysis which consists of substracting the syneresis liquid spectrum from that of the wet gel. The computer treatment reveals numerous weak and broad bands. Three of them, centred on 1050, 1318 and 1660 cm^{-1} respectively, are more intense.

The SAXS analyses allow us to calculate the radius of gyration for different wet gels (Table I). R_G increases in size with the gel opacity. All the scattering curves (Figs 6 and 7) exhibit a change in slope for H near $2\,nm^{-1}$ in the Porod region. These results confirm observations on gelation behaviour. The gels have a polymeric structure produced by aggregation of polymeric primary clusters. The slope for high values of H

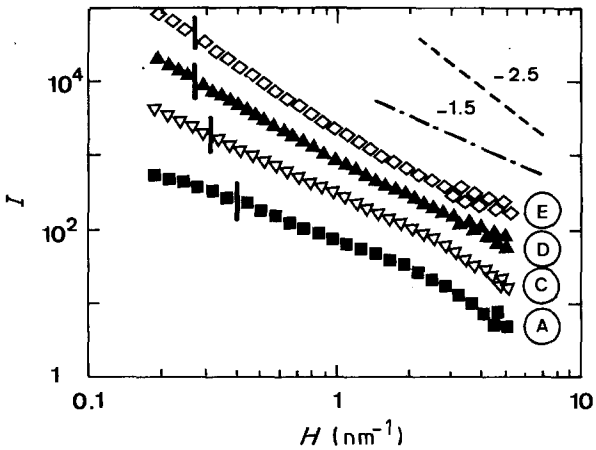

Figure 6 $I = f(H)$ for A, C, D and E ($I \equiv 2/R_G$).

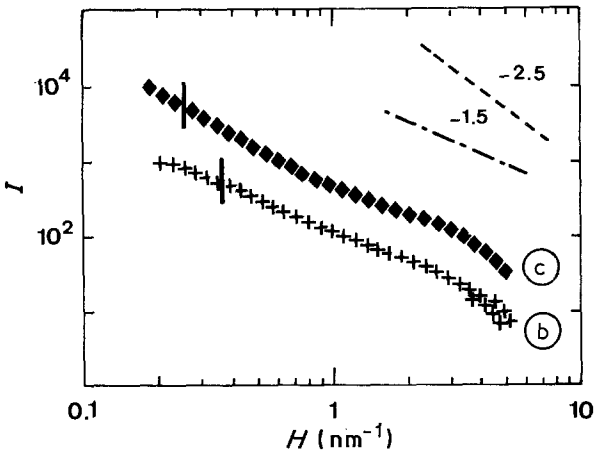

Figure 7 $I = f(H)$ for b and c ($I \equiv 2/R_G$).

is close to -2.5 except for gels D and E for which it is near to -1.5. For these last compositions (short gelation time), the cluster formation and aggregation could occur simultaneously leading to a less dense structure of the primary clusters. However, it must be underlined that this phenomenon is not observed with gel c which is instantaneously gelified but also obtained from more concentrated alkoxide solutions. In the $2R_G^{-1} - 2\,nm^{-1}$ range, the slope increases with the gel opacity from -1.5 for the transparent gels to -2.5 for the more opaque. The opacity of the wet gels increases as the acid concentration decreases. When the acidity of the medium increases the stability of the clusters towards aggregation also increases. As a consequence a less dense aggregated structure results. These aggregation differences can also explain why opacity corresponding to visible range increases as acid concentration decreases.

It must be noted that in the case of an aggregation of clusters generated by liquid phase extraction or sedimentation, the colloidal stability acts differently. The more stable the dispersion, the more dense the aggregate and the higher the fractal dimension [8].

Yoldas [4] suggests that, during zirconium alkoxide hydrolysis, localized condensation which occurs at higher water concentration can be prevented by introduction of acid. The acid requirement is found to be a function of the dilution and the water-to-alkoxide ratio. Our SAXS results are consistent with this analysis.

3.3. The xerogels

X-ray diffraction pattern shows that the dried gel is amorphous. Fig. 8 shows the Raman spectrum of the xerogel B. All the xerogels exhibit spectra which mainly consist of (i) a complex band with two maxima between 1000 and 1070 cm^{-1} and (2) weak and often broad bands at 520, 650, 780, 950, 1300, 1460 cm^{-1}.

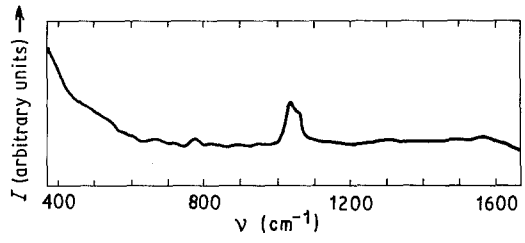

Figure 8 Raman spectrum of xerogel B.

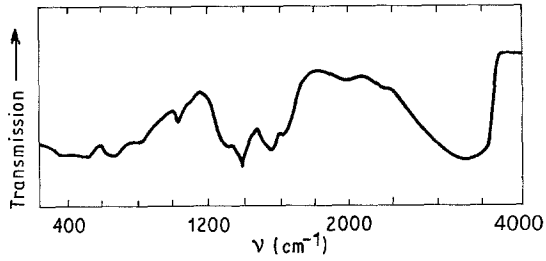

Figure 9 Typical IR spectrum for xerogels (KBr pellet technique).

The band situated at 1000 to 1070 cm^{-1} can be assigned either to the symmetric vibration of the nitrate ion ν_1 or to a vibration of the ZrOH group [9]. The symmetric vibration ν_1 is the only intense band active in Raman spectroscopy of the nitrate ion [10]. On the other hand the IR spectrum of the xerogels (Fig. 9) shows all the vibration bands of the nitrate ion which are IR active. In the range 950 to 1800 cm^{-1}, it is practically identical with the spectrum of the hydrated zirconium nitrate $Zr(NO_3)_4$, $5H_2O$ [11].

The hydrated zirconium nitrate $Zr(NO_3)_4$, $5H_2O$ or the hydrated zirconyl nitrate $ZrO(NO_3)_2$, $2H_2O$ exhibit IR spectra [11] showing a double band between 1000 and 1050 cm^{-1}. On the other hand the spectrum of the zirconyl chloride $ZrOCl_2$, $8H_2O$ in solid state [11] or in solution exhibits a single band situated at 1025 cm^{-1}. This band has been assigned to a vibration of the ZrOH group as it was previously demonstrated using a deuteration experiment [9].

The band located at 1050 cm^{-1} is probably due to the symmetric vibration of the nitrate ion and the band situated at 1025 cm^{-1} to a bending vibration of the ZrOH group. These assignments are supported by the structural evolution of the gels as a function of the temperature. The band at 1050 cm^{-1} really disappears in a temperature range corresponding to the thermal decomposition of the nitrates [12]. On the other hand the chemical bond Zr–OH seems to be very strong: the water departure occurs only with the crystallization phenomenon.

The weak 780 and 1460 cm^{-1} Raman bands can be assigned to vibrations of the nitrate ion. Thus both IR and Raman analyses demonstrate the presence of nitrate ion in the dried gel. It must be underlined that the spectra of the wet gels already showed the band at 1050 cm^{-1}. The zirconia gel retains the nitrate ions on its network.

The band at 520 cm^{-1} is certainly linked to a vibration of the Zr–O bond [9]. As will be described later, its intensity increases while that of 1025 and

TABLE I Electronic gyration radius R_G and visual appearance

Gel	R_G (nm)	Opacity
A	5.1	transparent
B	6.4	slightly opaque
C	6.8	opaque
D	7.7	very opaque
E	7.9	very opaque

Gel	R_G (nm)	Opacity
b	5.5	transparent ≡ A
c	8.0	opaque ≡ D

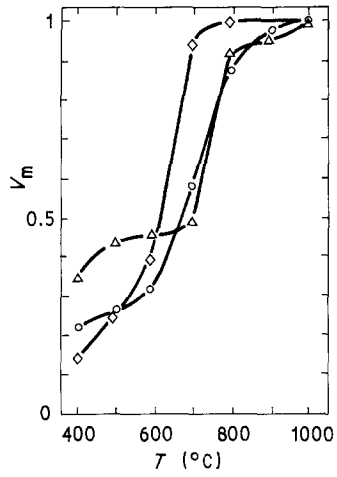

Figure 10 Volumetric fraction of monoclinic zirconia versus temperature for 2 h of treatment; gel a: ◇; gels b–d: ○; gel C: △.

1050 cm^{-1} bands decreases when the xerogel is heat treated. This band is probably related to the presence of zirconium hydroxyoxide compound.

3.4. The heat-treated gels

With thermal treatment the following crystallization sequence is observed using X-ray diffraction:

$$\text{amorphous} \rightarrow \begin{matrix}\text{metastable} \\ \text{tetragonal}\end{matrix} \rightarrow \text{monoclinic}$$

The crystallization of the xerogel is observed after a heat treatment for 2 h at 400° C. As the temperature increases the metastable tetragonal phase is transformed into monoclinic form. After 2 h at 1000° C this transformation is usually achieved.

DTA has been carried out at a heating rate of 10° C min^{-1}. The DTA curves exhibit exothermic peaks up to 400° C which are related to the oxidation of the organic groups. Around 500° C a very weak and broad peak can be observed. From various thermal treatments and X-ray diffraction analyses it can be deduced that this weak exothermic peak is produced by the crystallization of the amorphous material giving rise to metastable tetragonal phase. No peak related to monoclinic crystallization can be detected.

Various explanations are offered for the existence and the stability on temperature scale of the metastable phase [13]. Structural analogies between the amorphous and the tetragonal zirconia [14] can play a very important role in the formation of the metastable tetragonal phase. On the other hand, its thermal stability increases as the crystallite decreases [15]. This phase is stabilized by various ionic species such as OH^- [16].

To investigate the structural evolution of the various gels during thermal treatment, a semi-quantitative method was used. From the X-ray diffraction patterns the relative amount of monoclinic and tetragonal forms can be evaluated. This method is based on the measurement of the intensity of diffraction peaks of the metastable tetragonal (t) and monoclinic (m) phases. By modifying a relationship previously reported for mixtures of cubic and monoclinic zirconia [17] the volumetric fraction of the monoclinic form can be expressed:

$$V_m = \frac{1.603[I(1\,1\,\bar{1})_m]}{1.603[I(1\,1\,\bar{1})_m] + I(1\,1\,1)_t}$$

The evolution of V_m (Fig. 10) confirms the progressive formation of the monoclinic phase which starts above 400° C at the expense of the tetragonal form. The tetragonal–monoclinic transformation seems to be relatively regular for the gel a and is achieved at 800° C. Gels b to d and C behave differently: the monoclinic fraction does not change within the temperature ranges 300 to 600° C and 300 to 700° C, respectively.

No direct correlation can be obtained between the structural evolution of the gels and their composition or their opacity. This suggests that many parameters such as the texture of the gels or impurities (mineral as the nitrates and organic as carbon residues) can play a role on tetragonal–monoclinic conversion.

All the Raman spectra of the studied samples evolve qualitatively in the same way with temperature (Figs 11 and 12). As the temperature increases the intensity of the bands related to nitrates and ZrOH groups decreases. That fact clearly indicates the

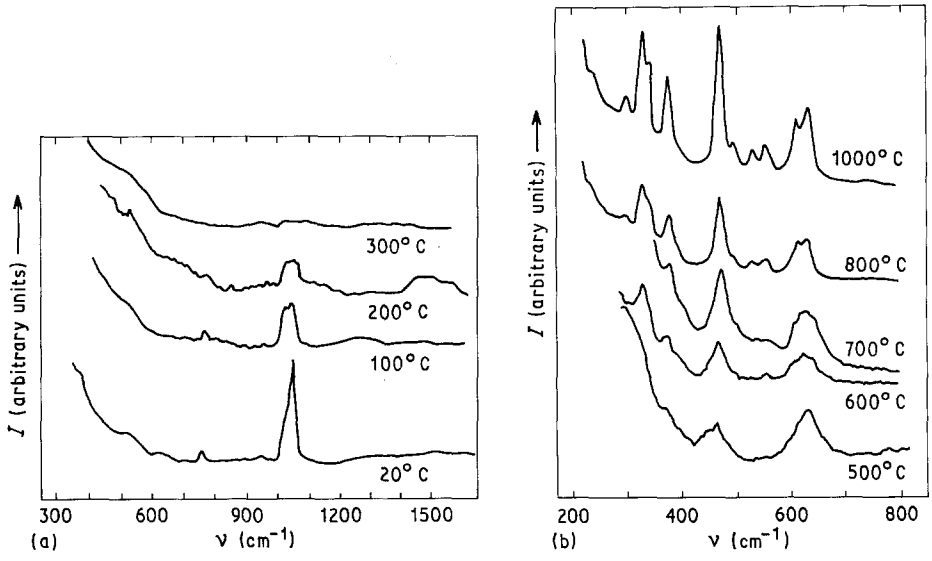

Figure 11 Raman spectra for thermally treated gel C: a) between 20 and 300° C; b) between 500 and 1000° C.

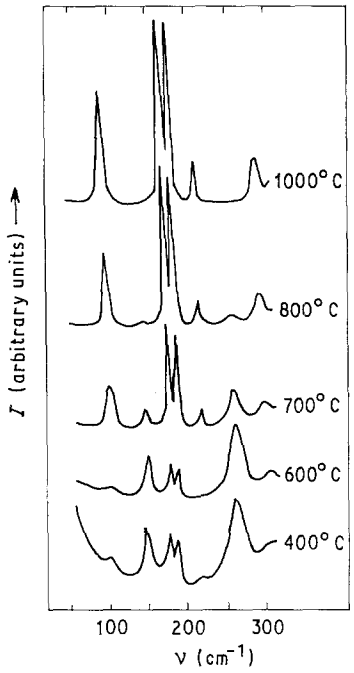

Figure 12 Raman spectra for thermally treated gel d in the frequency range 50 to 300 cm^{-1}.

dehydration of the gel. On the contrary, the intensity of the band located at 520 cm^{-1} and assigned to a vibration of the ZrO bond, increases.

As the gel crystallizes (above 400° C) the previously described bands vanish while two new broad bands located at about 475 and 630 cm^{-1} appear. Their intensities increase up to 600° C. Above this temperature their shape is modified: the half-height width decreases as the maximum intensity increases. Moreover, several other bands appear particularly on the low frequency side (Fig. 12). With respect to their temperature evolution these bands are assigned to the various ZrO_2 crystalline forms (Table II). Finally when the gel is heat treated for 2 h at 1000° C the recorded Raman spectrum is identical to that of the monoclinic zirconia [18].

The 475 cm^{-1} band is observed in the spectra of the two crystalline phases. The study of its shape evolution with temperature allows us to follow the tetragonal–monoclinic transformation. The result (Fig. 13) corroborates previous X-ray diffraction results.

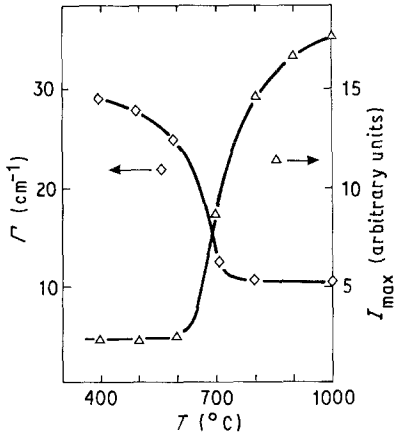

Figure 13 Evolution of the half-height width Γ and of the relative intensity of the 475 cm^{-1} Raman band versus temperature (gel d).

TABLE II Frequencies (cm^{-1}), intensities and assignment of the Raman bands

Amorphous gel		Metastable tetragonal phase		Monoclinic phase	
ν (cm^{-1})	I	ν (cm^{-1})	I	ν (cm^{-1})	I
520	vw	148	s	98	m
650	vw	263	s	178	vs
780	vw	400	sh	190	vs
950	vw	475	m	224	m
1025	m	630	m	310	mw
1050	m			340	s
1300	vw			355	m
1460	vw			385	m
				476	s
				503	w
				540	w
				560	w
				618	m
				640	m

(vs: very strong; s: strong; m: medium; w: weak; vw: very weak; sh: shoulder).

4. Conclusion

Zirconia gels are synthesized from a zirconium alkoxide precursor. The study of the alkoxide hydrolysis was performed using Raman spectroscopy. This reaction occurs immediately after the reactants are mixed. From SAXS analyses it appears that the gelation could be regarded as a resulting phenomenon of an aggregation of primary clusters produced just after the mixture preparation. The gelation is here linked to both chemical and physical mechanisms.

The structural study of the gel led us to think that the xerogel is probably an amorphous zirconium hydroxyoxide. Nitrate ions are strongly bound to the xerogel network.

The xerogel crystallization in metastable tetragonal zirconia is obtained after a thermal treatment at 400° C for 2 h. It must be noted that the first phase which appears is the upper temperature phase. This phenomenon is probably related to the initial structure of the amorphous compound. This structure may be "open" as that of glass. In this way the crystalline form which appears first, is that structurally favoured independently of its thermal stability.

When the temperature increases a progressive transformation to stable monoclinic zirconia occurs. After 2 h of thermal treatment performed at 1000° C, the material mainly consists of monoclinic zirconia.

References

1. N. CLAUSSEN, M. RUHLE and A. H. HEUER (eds) "Science and Technology of Zirconia II", "Advances in Ceramics", Vol. 12 (American Ceramic Society, Columbus, USA, 1984).
2. D. C. BRADLEY and D. G. CARTER, *Can. J. Chem.* **39** (1961) 1434.
3. *Idem., ibid.* **40** (1962) 15.
4. B. E. YOLDAS, *J. Mater. Sci.* **21** (1986) 1080.
5. T. ASSIH, A. AYRAL, M. ABENOZA and J. PHALIPPOU, *J. Mater. Sci.* **23** (1988) 3326.
6. J. C. POUXVIEL, J. P. BOILOT, A. LECOMTE and A. DAUGER, *J. Physique* **48** (1987) 921.
7. D. W. SCHAEFER, J. P. WILCOXON, K. D. KEEFER, B. C. BUNKER, R. K. PEARSON, I. M. THOMAS and D. E. MILLER, in Proceedings of AIP

Conference 154; Physics and Chemistry of Porous Media II (American Institute of Physics, NY., USA, 1987) p. 63.
8. E. DICKINSON, *J. Colloid. Interface Sci.* **118** (1) (1987) 286.
9. K. BURKOV, G. V. KOZHEVNIKOVA, L. S. LILICH and L. A. MYUND, *Russ. J. Inorg. Chem.* **27** (6) (1982) 804.
10. D. V. LUU, M. ABENOZA, A. ARMENGAUD and J. M. PASTOR., *Spectrochim. Acta* **33A** (1977) 213.
11. R. A. NYQUIST and R. O. KAGEL, "Infrared Spectra of Inorganic Compounds" (Academic Press, New York, 1971).
12. J. P. LANGERON in "Nouveau Traité de Chimie Minérale – tome IX" (Masson, Paris, France, 1963) p. 635.
13. T. KOSMAC, R. GOPALA KRISHNAN, V. KRASEVEC and M. KOMAC, *J. Physique* **47** supplément au no 2, colloque C1 (1986) 43.
14. J. LIVAGE, K. DOI and C. MAZIERES, *J. Amer. Ceram. Soc.* **51** (6) (1968) 349.
15. R. C. GARVIE, *J. Phys. Chem.* **69** (4) (1965) 1238.
16. R. CYPRES, R. WOLLAST and J. RANCQ, *Ber. Dtsch. Keram. Ges.* **40** H9 (1963) 527.
17. D. L. PORTER and A. H. HEUER, *J. Amer. Ceram. Soc.* **62** (5–6) (1978) 298.
18. V. G. KERAMIDAS and W. B. WHITE, *ibid.* **57** (1) (1974) 22.

Received 22 November 1988
and accepted 2 May 1989